Journal of Food Engineering 108 (2012) 194–200

Contents lists available at ScienceDirect

Journal of Food Engineering

journal homepage: www.elsevier.com/locate/jfoodeng

Studies on banana fruit quality and maturity stages using hyperspectral imaging

P. Rajkumar [a,*], N. Wang [b], G. EImasry [b], G.S.V. Raghavan [b], Y. Gariepy [b]

[a] Trainee at McGill University, Canada & Associate Professor, Dept. of Food & Agrl. Process Engineering, AEC&RI, TNAU, Coimbatore 641003, India
[b] Dept. of Bioresource Engineering, Macdonald Campus of McGill University, Canada H9X 3V9

ARTICLE INFO

Article history:
Received 30 January 2010
Received in revised form 2 May 2011
Accepted 3 May 2011
Available online 11 May 2011

Keywords:
Non-destructive
Hyperspectral
Maturity
PLS
MLR
PCA

ABSTRACT

Banana fruit quality and maturity stages were studied at three different temperatures, *viz.,* 20, 25, and 30 °C by using hyperspectral imaging technique in the visible and near infrared (400–1000 nm) regions. The quality parameters like moisture content, firmness and total soluble solids were determined and correlated with the spectral data. The spectral data were analyzed using the partial least square analysis. The optimal wavelengths were selected using predicted residual error sum of squares. The principal component analysis was also used to test the variability of the observed data. By using multiple linear regressions (MLR), models were established based on the optimal wave lengths to predict the quality attributes. The coefficient of determination was found to be 0.85, 0.87, and 0.91 for total soluble solids, moisture and firmness of the banana fruits, respectively. The change in TSS and firmness of banana fruits stored at different temperatures, *viz.,* 20, 25, and 30 °C during the ripening process followed the polynomial relationships and the change in moisture content followed a linear relationship at different maturity stages.

1. Introduction

Banana is one of the important fruits consumed all over the world. Optimum ripening stage for banana bunches/fruits is required to maintain the quality and to get good market price, followed by correct handling and packing of the fruit. The fruit ripening and maturity standards vary from country to country depending on the expected green life required by the fruit before ripening takes place. The quality attributes of a fruit are categorized as sensory, hidden and quantitative. The sensory attributes are colour, glossiness, size, shape, defects, flavour, texture (firmness, crispiness and toughness) and taste. The hidden attributes are nutritive values, presence of dangerous contaminants and poisonous materials. The quantitative parameters are those, which contribute to the overall food quality. Various methods have been used to determine the maturity stages of banana but the techniques adopted are destructive involving determination of pulp to peel ratio and firmness of the fruit (Ramma et al., 1999). Therefore, any technology that can classify the fruits based on colour, texture, taste, flavour and nutritive value would assure more fruit quality and consistency which in turn increases the consumer acceptance and satisfaction. Also, the processing industry will be under healthy competition with more profitability (Lu and Ariana, 2002).

Now a days fruits are sorted either manually or mechanically based on the external quality features. But the internal quality attributes such as moisture content, total soluble solids and firmness are also increasingly important in the growing trend. Most instrumental methods used to measure these properties are destructive involving manual work. The non-destructive measurement of the internal quality attributes of the fruit is becoming important for the consumers and the industry as a whole.

Machine vision technology is becoming popular in the field of pre and post harvest product quality, safety detection, sorting, and process automation, since they can recognize size, shape, colour, and texture of objects and also the numerical attributes of the objects. In the machine vision technology series, hyperspectral imaging has emerged as a powerful technique, which combines visible imaging and spectroscopy to acquire both spatial and spectral information from an object. Because of the combined features, the hyperspectral imaging technique can greatly enhance the capability to identify and detect various chemical constituents of the fruit along with their spatial distributions. An imaging camera receives the light reflected from the object surface and converts the light into electrical signals using a charged coupled device (CCD), which are solid state; silicon based devices and is available in linear and area array configurations. The CCD detectors have two dimensional arrays and a spectrograph allows simultaneous recording of a line of spatial and a multiple of spectral information.

Preliminary study on identifying normal and abnormal poultry carcasses using hyperspectral imaging technique was conducted by Lu and Chen (1998), since then the technique has been redesigned to evaluate the reflectance and fluorescence images of agricultural products (Kim et al., 2002b). This hyperspectral imaging technique has been successfully used for the quality sorting of

* Corresponding author. Tel.: +91 9443046665; fax: +91 4225511455.
E-mail address: prajtnau@yahoo.co.in (P. Rajkumar).

0260-8774/$ - see front matter © 2011 Elsevier Ltd. All rights reserved.
doi:10.1016/j.jfoodeng.2011.05.002

Nomenclature

a	number of partial least square factors
a_0,β, a_N	regression coefficients
CCD	charged coupled device
I_A	acquired hyperspectral image
I_D	dark image
IR	infrared
I_W	white reference
MLR	multiple linear regression
N	number of optimal wavelength
NIR	near infrared
nm	nano meter
P	orthogonal projection axes
PC	principal component
PLS	partial least square
R	reflectance
TSS	total soluble solids
VIR	visible infrared
T	wavelength scores
$\hat{Y}$	predicted value of the quality attribute
λ	wavelength

strawberry (EImasry et al., 2007), detection of defects in apples (Elmasry et al., 2008; Kim et al., 2002a; Mehl et al., 2004), detection of contamination of poultry (Lawrence et al., 2003; Park et al., 2003), food quality evaluation and safety inspection (Lu and Chen, 1998).

The hyperspectral imaging technique has not been fully applied for online quality grading due to its time consumption for acquiring the image (Mehl et al., 2002). But, Lee et al. (2005) reported that this problem could be overcome by using only the optimal wavelength to acquire the image and then the online sorting could be done by using multispectral imaging technique. Shmulevich et al. (2003) reported that the correlation coefficients for the prediction of textural properties using non-destructive methods varying from 0.53 to 0.84 for different fruits.

The machine vision technology has many advantages such as the method is fairly accurate, non destructive, and yields consistent results. Therefore the technique can improve the food industrial productivity, reduction in cost and make the process safer with better quality to the consumers. Besides imaging objects in the visible region, the hyperspectral imaging can also be used to inspect the objects in light invisible to human eyes such as ultraviolet, near infra red, and infrared (IR) regions. The acquired image can be useful in predicting plant maturity, disease or stress states. Also, this technique can be used to classify the objects based on variety, ripeness, quality, composition, and contaminations.

Hence, a study was undertaken to acquire the hyperspectral image of banana fruits at different ripening/maturity stages and stored at different temperatures, *viz*., 20, 25, and 30 °C to develop the calibration models for the prediction of quality parameters based on hyperspectral data. Also to develop a relationship between selected fruit quality attributes at different temperatures.

2. Methods and materials

Unripe banana fruits without any damage were selected and stored at different temperatures, *viz*., 20, 25, and 30 °C with 70% relative humidity. Two hundred and seventy fruits were divided into 6 groups for representing ripening stages from 1 to 6 with each group consists of 15 banana fruits. The experiment was replicated thrice. The group was selected randomly for hyperspectral imaging and subsequent biochemical quality parameters on alternate days. The tested fruits in each ripening stage were randomly divided into two sub groups. The sub group 1 consisted of 10 fruits used as a training set for developing partial least square model. The sub group 2 consisted of 5 fruits used for validation of the training models. The results are for the fruits stored at 20 °C.

2.1. Hyperspectral image acquiring system

A hyperspectral image acquiring system (Fig. 1) consists of four important components, *viz*., a spectrograph (ImSpector V10E, Optikon Co., Canada) coupled with a standard C-mount zoom lens, a charged couple device (CCD) camera (PCO – 1600, Pco. Imaging Germany), two 50 W halogen lamps fitted with an angle of 45° to illuminate in the camera's field of view, and a fruit holding platform surrounded with a white nylon cube tent. The exposure time for the data acquisition in the sensitivity range of 400–1000 nm were fixed as 200 ms for the whole experiment. The distance between the CCD camera lens and the surface of the banana was fixed as 35 cm. The images were recorded with a spatial dimension of 400×400 pixels and with 826 spectral bands from 400 to 1000 nm. For image acquisition, hypervisual imaging analyzer (Pro vision Technologies, Stennis Space Center, USA) was used.

The acquired images were processed using Environment for visualizing Images (ENVI 4.2) software (Research Systems Inc., Boulder Co., USA). Initially, the acquired images were corrected with a white and a dark references. The corrected image (Ic) is estimated as follows:

$$I_C = \frac{I_A - I_D}{I_W - I_D} x100 \quad (1)$$

where, I_A is the acquired hyperspectral image, I_D is the dark image recorded by closing the camera lens completely and turning off the external light source, I_W is the white reference image with 99% reflectance using Teflon white board. The experiment was replicated thrice to get standard deviations. The corrected images were used for the extraction of information about spectral properties, selection of effective wavelengths and model prediction with biochemical contents.

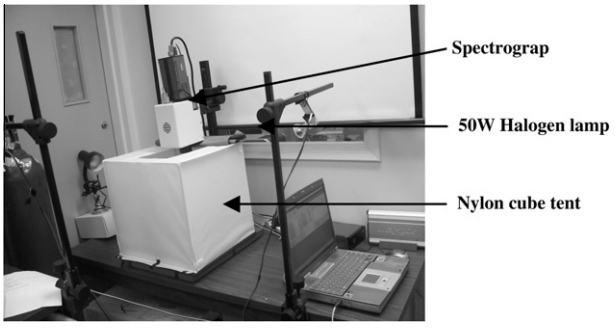

Fig. 1. Hyperspectral imaging system in operation.

2.2. Banana quality parameters

The quality parameters of banana fruit, *viz.*, total soluble solids, moisture content and firmness were measured and the values were used for the development of prediction model using spectral data. The total soluble solids (TSS) were determined using a refractometer with a range of 0–32°Brix (Model No. ATC-1090, Atago Co. Ltd., Japan). The TSS (°Brix) of the banana pulp was measured by dividing the fruit into three equal parts (length wise). From each part, ten gram sample was pulped using pestle and mortar. Then the pulped samples were used to find the TSS and reported as a mean of three replications. The moisture content was determined by drying the samples at 70 °C to constant weight using hot air oven.

The firmness of banana fruits was measured using Universal testing machine (Instron Corp., USA; Model – 4500). The fruit was cut into 5 cm length and the firmness of the pulp was measured with a cylindrical Teflon probe of 0.5 cm diameter at a crosshead speed of 10 mm/min. The firmness value was recorded in terms of Newton and reported as a mean of 3 readings.

2.3. Hyperspectral data analysis

Prediction model between the spectral reflectance and the quality parameters (Moisture content, TSS and firmness) of the fruits was developed by using partial least squares (PLS) analysis (GRAMS/AI – Thermo Electron Corp., Salem New Hampshire, USA). The reflectance values at 826 wavelengths of the fruits were taken as predicting variables X matrix ($N_{\text{fruits}} \times K_{826\ \text{wavelengths}}$) and the quality attributes were taken as dependent variables Y matrix ($N_{\text{fruits}} \times 1$). The PLS models are generally used to set up the multivariate model based on two data sets of the same object/sample namely spectral and biochemical values. The PLS can transfer the large set of highly correlated experimental data into independent latent variables or factors.

Using PLS algorithm, the predicted value of the attribute of interest $\hat{Y}$ was determined as follows (Geladi and Kowalski, 1986):

$$\hat{Y} = T_a\beta \tag{2}$$

where, $\hat{Y}$ is the predicted value of the quality attribute, T is the wavelength scores, '$_a$' is the number of PLS factors, and β is the regression coefficient. The optimal number of latent variables for establishing the calibration model was determined based on the predicted residual error sum of squares (PRESS).

2.4. Optimal wavelengths selection and multiple regression models

Generally, it is important to select the wavelengths, which contribute to the quality attribute of the product. Therefore, the highest absolute value of the β-coefficients correspond to the wavelengths obtained from the PLS calibration model was selected and used as the optimal wavelengths. Then these selected optimal wavelengths were used to establish multiple linear regression models using MATLAB (MATLAB 7.0, Release 14, The Math Works, Inc., Natick, MA, USA) as follows:

$$\hat{Y} = a_0 + \Sigma_{N-1}^{N} a_N R_{\lambda N} \tag{3}$$

where, $\hat{Y}$ is the predicted value of the quality attribute, N is the number of optimal wavelengths a_0 and a_N are the regression coefficients, and $R_{\lambda N}$ is the reflectance at a wavelength λ corresponding to the N^{th} term in the model.

To determine the reliability of the selected wavelengths representing different ripening/maturity stages, principal component analysis (PCA) was conducted on the reflectance spectra data. The PCA transforms the acquired data set into a new coordinate system with the greatest variance of the data set projected in the first coordinate (also called the first principal component) and the second greatest variance on the second coordinate and so on. The PCA is mainly used in dimensional reduction of the acquired data set while retaining the important characteristic, which contributes most of the variance.

3. Results and discussion

3.1. Spectral reflectance of the banana

The average spectral reflectance in the range of 400–1000 nm collected from the banana fruits at different maturity stages from 1 to 6 at different temperatures, *viz.*, 20, 25, and 30 °C are shown in Figs. 2–4. The banana fruits at 1 and 2 stages showed that the moisture content influenced the formation of characteristic absorption bands. The reflectance values were comparatively lower in matured fruits representing the stages 4, 5, and 6 when compared to the banana fruits representing at early stages (1–3). The fruits had three broad band absorptions in the maturity stages of 1–3 around 450, 680, and 960 nm regions.

The presence of chlorophyll pigment could be observed in the spectral range of 670–710 nm for the banana fruits stored at three different temperatures. But the presence of chlorophyll pigment (maturity stages 1 and 2) was higher in the fruits stored at 20 °C compared to the fruits stored at 25 °C and 30 °C. This absorption was not seen in the matured stages of 4–6, since the fruit turned into yellow colour and the chlorophyll was degraded completely. Among the temperatures, the chlorophyll pigment absorption was lower in the stage 1 of the banana fruit stored at 30 °C showing fast changes in the colour compared to the fruits stored at lower temperatures of 25 and 20 °C. These observed values are similar to the spectral band absorption values reported by Abbott et al. (1997) and EImasry et al., (2007) for apples, Lu and Peng (2006) for peach fruits, respectively. The relative reflectance representing sugar absorption bands were lower for the mature and over mature fruits (stages 4, 5, and 6) compared to the early stages of 1, 2, and 3 due to higher sugar content in the fruit stored at all the three temperatures.

The spectral bands from 800–960 nm showed the water content of the fruit, which clearly demarcated the stages based on the amount of moisture available in the fruits. Since, the unripe fruit peel had higher moisture and correspondingly the reflection was also higher for the unripe fruits representing stages 1 and 2. The reflection was lower in the fruits representing the stages of 3, 4, 5, and 6 due to lower moisture content in the fruit peel. Since, water content is the most abundant constituent in the pulp and

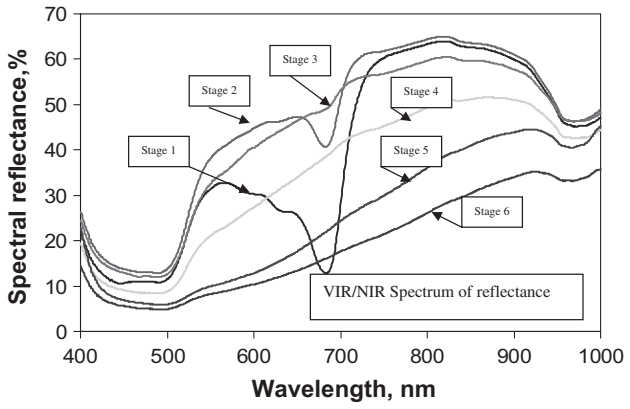

Fig. 2. Hyperspectral reflectance of VIR/NIR spectrum at different maturity stages of banana fruits stored at 20 °C.

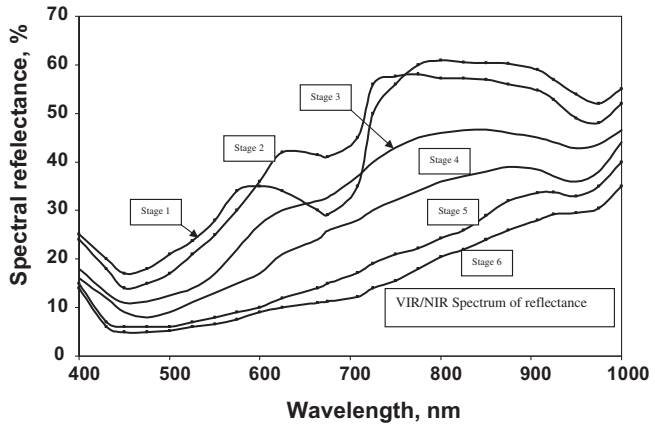

Fig. 3. Hyperspectral reflectance of VIR/NIR spectrum at different maturity stages of banana fruits stored at 25 °C.

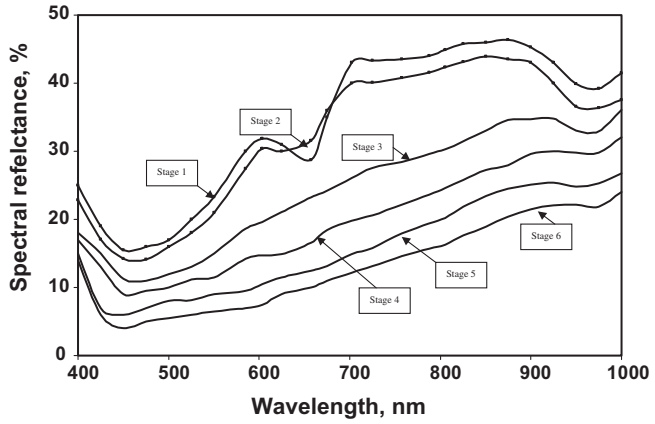

Fig. 4. Hyperspectral reflectance of VIR/NIR spectrum at different maturity stages of banana fruits stored at 30 °C.

peel of banana. The water content increases in the pulp during the onset of ripening due to respiratory break down of starch and osmotic movement of water from peel to pulp. Simultaneously, the water is also lost from the peel externally due to transpiration until ripening process ceases. At this stage, the peel tissue prevents further water losses.

The overall difference in reflection spectra of the banana fruits might be due to the noticeable changes that took place simultaneously during ripening such as change in colour, TSS, firmness and moisture content. Various enzymatic reactions are involved during the colour change process, where the ratio of sugar to starch increases and then a characteristic aroma is developed. Therefore, the peel becomes spotted brown and then completely brown and the pulp loose its firmness, white texture becomes gelatinous and correspondingly the absorption bands are also changing during these processes. A little variation in the present results for banana fruits compared to the results reported by EImasry et al., (2007) might be due to the difference in the spectral absorption characteristics of strawberry compared to banana fruits.

3.2. Optimal wavelengths selection and multiple regression models

The PLS calibration models were established for the banana fruits using the average spectra of the whole spectral range of 826 wave bands. The number of latent factors for PLS model for predicting the maturity stages in terms of quality parameters was determined by selecting the lowest value of predicted residual errors sum of squares (PRESS). The lowest number of latent factors

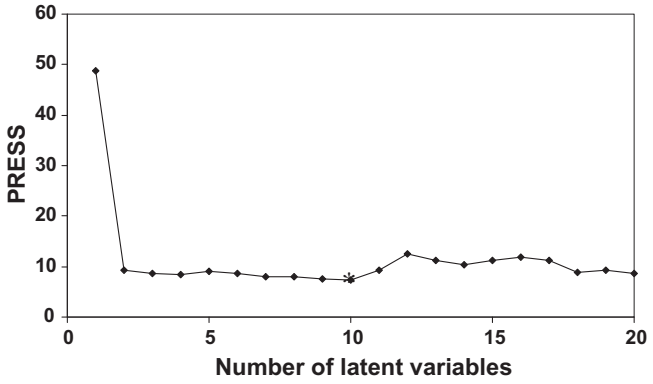

Fig. 5. Optimal number of loadings using PLS based on Predicted residual error sum of squares.

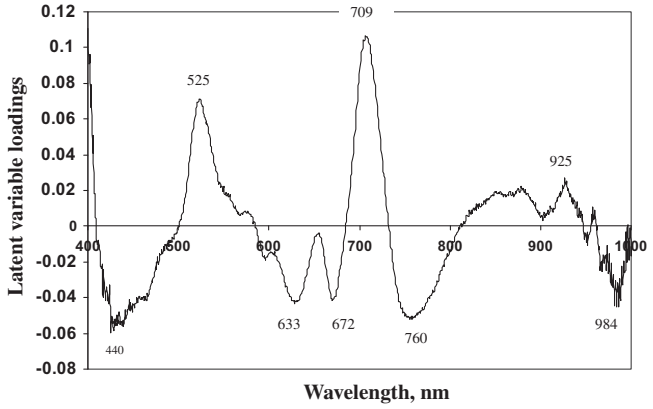

Fig. 6. Optimal wavelengths for predicting quality attributes of banana fruits.

was found to be 10 for the selection of optimum wavelengths to predict the maturity stages of banana fruits as shown in Fig. 5.

The PRESS started decreasing from the higher value to the lower values until its lowest value matching with the ideal number of latent factors. After this point, the PRESS started increasing with increase in number of latent factors but correspondingly the performance of the model was reduced. The β coefficient plot extraction is shown in the figure for the selection of optimal wave bands for the prediction of maturity stages of banana fruits (Fig. 6).

From the β coefficient of PLS, (Eq. 2), the optimum wavelengths for predicting the maturity stages of banana fruits with internal quality attributes such as moisture, TSS and firmness were found to be 440, 525, 633, 672, 709, 760, 925, and 984. The selected optimal wavelengths were corresponding to the highest absolute value of the β coefficient irrespective of the sign.

The principal component analysis conducted on the selected optimal wavelengths showed that the first two components explained 99.88% (PC1–89.88% and PC2–8.38%) of the difference in maturity stages of banana fruits (Fig. 7). The observed values were distinguished clearly into different groups. It was also observed that the selected wavelengths showed a good potential of discriminating the ripening/maturity stages of banana fruits.

The multiple linear regression (MLR) was conducted to predict the moisture content, TSS and firmness based on the selected spectral data.

3.3. Prediction of total soluble solids (TSS)

The predicted TSS based on spectral values and observed TSS based on experiment is shown in Fig. 8. The values were analyzed

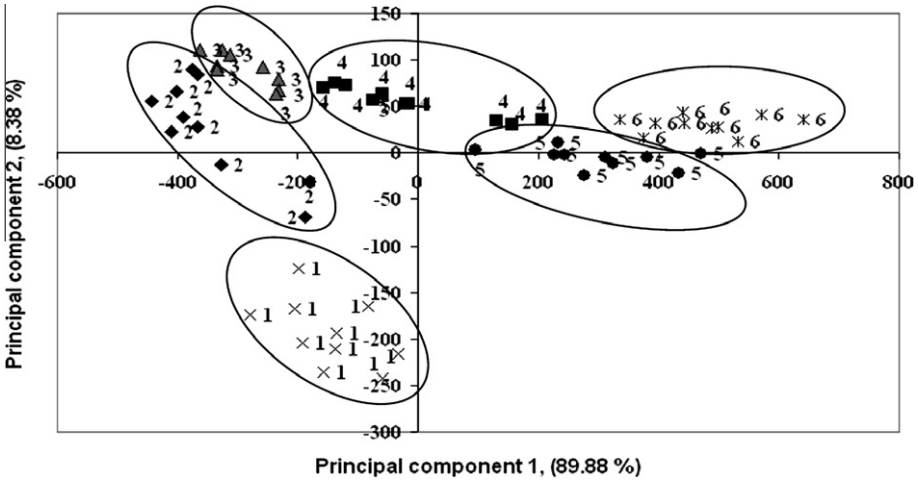

Fig. 7. Principal component analysis of the selected wavelengths.

using MLR. The TSS prediction was found to be within the seven optimal wavelengths. The MLR model indicated that the calibration model with 10 PLS factors were adequate. The coefficient of determination (R^2) was found to be 0.85, signifying good correlation between the predicted TSS using selected wavelengths and the measured TSS during the ripening/maturity stages for the fruits stored at 20 °C. The validation data had a coefficient of determination of 0.89 and the validation data also indicated that the calibration model with 10 PLS factors were appropriate. Williams and Norris (1987) identified the absorbance band for sugar (838, 888, 913, 978, and 1005 nm) and starch (878, 901, 918, 979, 1030, and 1053 nm) in the near infrared regions contributing TSS. Martinsen and Schaare, (1998) concluded that the hyperspectral imaging was found to be a promising technique to determine the soluble solids distribution in kiwi fruit. The present study results are in comparable with the results of Ito (2002) and EImasry et al., (2007) for strawberry fruits. From the statistical analysis of the measured TSS, it was observed that the TSS had increased significantly up to the 4th stage of maturity and then started decreasing significantly at 5th and 6th stages for the fruits stored at 20 °C (Table 1). Whereas at 25 °C and 30 °C, the TSS increased up to 3rd and 2nd stages, respectively due to fast ripening process (Tables 2 and 3). The change in TSS of banana fruits stored at different temperatures, *viz*., 20, 25, and 30 °C during the ripening process were analyzed at different maturity stages. The following polynomial relationships were obtained.

$$TSS_{(20^\circ C)} = -0.809x^2 + 6.104x + 8.715 \quad R^2 = 0.9023 \tag{4}$$

$$TSS_{(25^\circ C)} = -0.786x^2 + 5.672x + 9.866 \quad R^2 = 0.9831 \tag{5}$$

$$TSS_{(30^\circ C)} = -0.518x^2 + 3.263x + 12.912 \quad R^2 = 0.4387 \tag{6}$$

3.4. Prediction of moisture content

A good correlation between observed and predicted moisture based on selected absorption bands for the whole data set of the banana fruits. The coefficient of determination for the calibration and validation models was found to be 0.81, and 0.9, respectively (Fig. 9) for the fruits at 20 °C. Eight wavelengths (440, 525, 633, 672, 709, 760, 925, and 984) were needed to obtain the moisture prediction in banana fruits at different ripening/maturity stages. Williams and Norris (1987) reported the water absorption bands for the peach fruits were 834, 938, 958, 978, 986, and 994 nm, whereas Lu and Peng (2006) reported that the water absorption band was found to be at 950 nm using hyperspectral imaging technique for peach fruits. But the reported results with the present study are found to be varying due to the difference in the spectral absorption characteristics of banana fruits. The statistical analysis of the measured moisture content showed that there was a significant difference in the moisture contents at stages 1, 2, and 3. But at stages 4 and 5, the moisture content of the fruits were on par with each other and at stage 6, the fruits had significantly higher amount of moisture in the pulp due to respiratory break down of starch and degradation of fruit. From the Tables 1–3, it is understood that the moisture content increase with increase in ripening and also increase with increase in storage temperatures due to respiratory break down of starch and osmotic movement of water from peel to pulp. The change in moisture content of banana fruits stored at different temperatures, *viz*., 20, 25, and 30 °C during the ripening process were analyzed at different maturity stages. A linear relationship was found between moisture content and maturity stages of banana fruits stored at different temperatures.

$$M.C._{(20^\circ C)} = 1.843x + 72.935 \quad R^2 = 0.9321 \tag{7}$$

$$M.C._{(25^\circ C)} = 2.167x + 73.123 \quad R^2 = 0.9933 \tag{8}$$

$$M.C._{(30^\circ C)} = 1.522x + 78.115 \quad R^2 = 0.9519 \tag{9}$$

3.5. Prediction of firmness

The coefficients of determinations for the training and validation data set of firmness of the fruits were found to be 0.91 for the fruits stored at 20 °C. The results showed that the selected eight spectral wavelengths were required to predict the fruit firmness, representing different ripening/maturity stages (Fig. 10). The measured firmness were statistically analyzed and presented in Tables 1–3. The results showed that there

Table 1
Quality parameters of the banana fruits at 20 °C.

Banana fruits	Stage1	Stage2	Stage3	Stage4	Stage5	Stage6
Firmness	9.95 ± 0.44a	6.33 ± 0.66b	5.89 ± 0.49c	5.78 ± 0.56d	4.33 ± 0.34e	1.14 ± 0.32f
TSS	13.92 ± 0.13a	18.42 ± 0.44b	18.55 ± 0.52c	20.3 ± 0.63 cd	19.92 ± 0.29e	15.77 ± 0.32f
Moisture	74.87 ± 0.73a	76.82 ± 0.36b	78.93 ± 0.81c	79.70 ± 0.75d	79.97 ± 0.72de	85.28 ± 0.48f

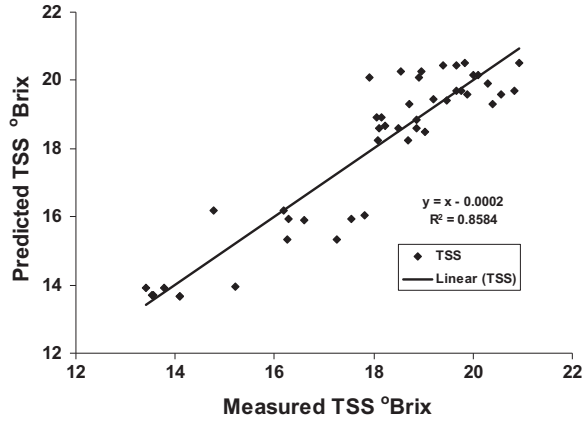

a) Training set for TSS

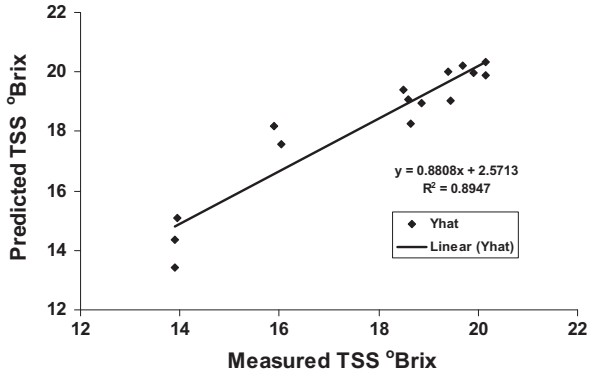

b) Validation set for TSS

Fig. 8. Measured and predicted TSS for training and validation sets using selected spectral data for the fruits stored at 20 °C.

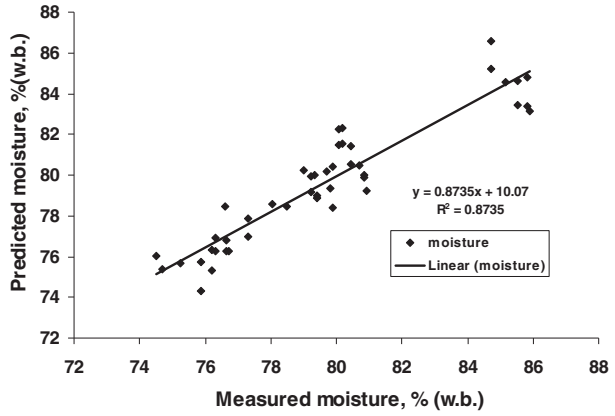

a) Training set for moisture content

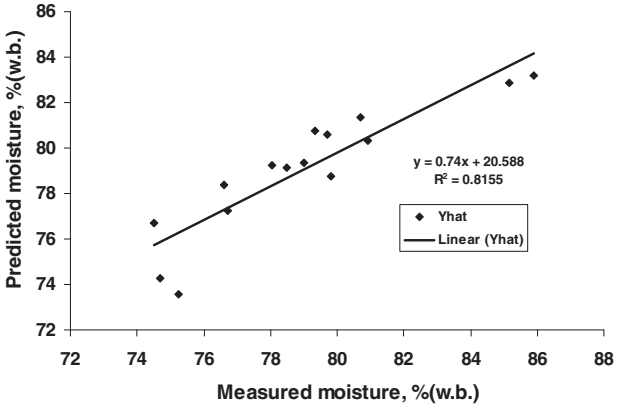

b) Validation set for moisture content

Fig. 9. Measured and predicted moisture for training and validation sets using selected spectral data for the fruits stored at 20 °C.

Table 2
Quality parameters of the banana fruits at 25 °C.

Banana fruits	Stage1	Stage2	Stage3	Stage4	Stage5	Stage6
Firmness	9.56 ± 0.31a	5.12 ± 0.50b	4.93 ± 0.49c	3.25 ± 0.21d	2.98 ± 0.18e	1.10 ± 0.11f
TSS	14.75 ± 0.27a	17.99 ± 0.35b	20.12 ± 0.29c	19.52 ± 0.24d	18.87 ± 0.34e	15.53 ± 0.36f
Moisture	75.15 ± 0.38a	77.21 ± 0.54b	79.86 ± 0.89c	82.36 ± 0.83d	83.79 ± 0.61d	85.87 ± 0.63e

Table 3
Quality parameters of the banana fruits at 30 °C.

Banana fruits	Stage1	Stage2	Stage3	Stage4	Stage5	Stage6
Firmness	7.91 ± 0.16a	3.98 ± 0.66b	2.89 ± 0.49c	1.46 ± 0.56d	1.28 ± 0.34e	1.02 ± 0.32f
TSS	14.02 ± 0.24a	20.02 ± 0.44b	18.75 ± 0.52c	15.96 ± 0.63d	15.11 ± 0.29e	14.97 ± 0.32f
Moisture	78.86 ± 0.41a	81.54 ± 0.56b	83.13 ± 0.78c	85.02 ± 0.65d	85.12 ± 0.52de	86.99 ± 0.31f

was a significant difference in firmness of banana fruits at each stage of ripeness/maturity.

Also, the firmness values were significantly decreased with increase in ripening process and increase in storage temperatures. The change in firmness of banana fruits stored at different temperatures, *viz*., 20, 25, and 30 °C during the ripening process at different maturity stages was found to be in polynomial relationships Eq. (10–12.) The prediction of firmness is an important textural property of banana, which directly influences the shelf life and consumer acceptance. The chlorophyll and water content are related to the fruit firmness of the fruit.

4. Conclusions

The hyperspectral imaging study could be used as a non destructive method to distinguish the banana fruit ripening/maturity stages at different temperatures. The PLS model showed that 10 latent factors could be used to select the optimal wavelength based on beta coefficients. Eight wavelengths were required to predict the maturity stages of banana fruits representing the quality attribute in terms of total soluble solids, moisture content and firmness. The multiple linear regression models could be used for

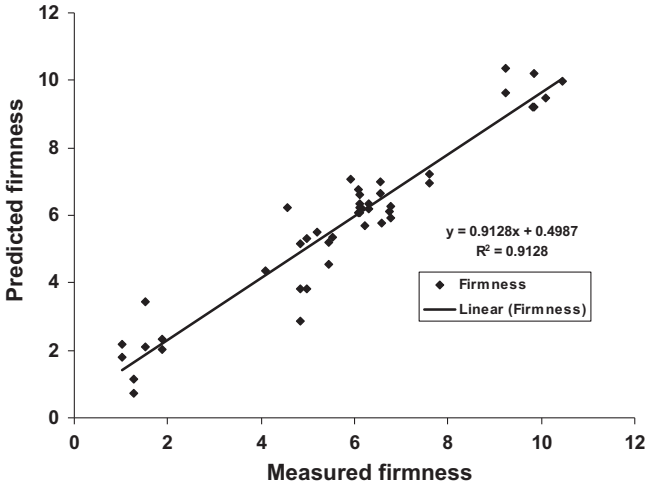

a) Training set for firmness

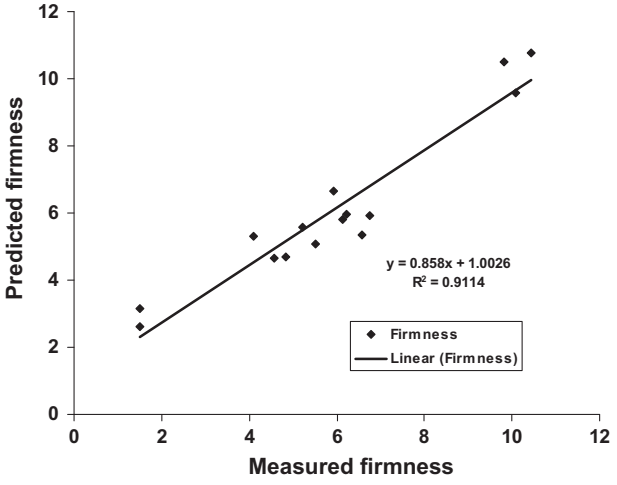

b) Validation set for firmness

Fig. 10. Measured and predicted firmness for training and validation sets using selected spectral data for the fruits stored at 20 °C.

establishing the prediction model for moisture, TSS and firmness using the selected optimal wavelengths. The ripening processes accelerate with increase in temperature. The change in TSS and firmness of banana fruits stored at different temperatures, *viz*., 20, 25, and 30 °C during the ripening process were found to be following the polynomial relationships. The change in moisture content of the banana fruits was found to be following a linear relationship at different maturity stages.

Acknowledgement

The authors wish to acknowledge the financial support given by Canadian International Development Agency and AICRP on Post Harvest Technology, India.

References

Abbott, J.A., Lu, R., Upchurch, B.L., Stroshine, R.L., 1997. Technologies for nondestructive quality evaluation of fruits and vegetables. In: Janick, J. (Ed.), Horticultural Reviews. John Wiley & Sons Inc. Vol. 20, pp. 1–120, ISBN:0 471 18906 5.

Elmasry, G., Wang, N., Vigneault, C., Quio, J., Elsayed, A., 2008. Early detection of apple bruises on different background colours using hyperspectral Imaging. LWT – Food Science and Technology 41 (2), 337–345.

Elmasry, G., Wang, N., Elsayed, A., Ngadi, M., 2007. Hyperspectral Imaging for nondestructive determination of some quality attributes of strawberry. Journal of Food Engineering 81 (1), 98–107.

Geladi, P., Bruce Kowalski, R., 1986. An example of 2-block predictive partial least-squares regression with simulated data. Analytica Chimica Acta 185, 19–32.

Lawrence, K.C., Windham, W.R., Park, B., Buhr, R.J., 2003. Hyperspectral imaging system for identification of fecal and ingesta contamination on poultry carcasses. Journal of Near Infrared Spectrascopy 11 (4), 269–281.

Lee, K.J., Kang, S., King, M.S., Noh S.H., 2005. Hyperspectral imaging for detecting defect on apples. ASAE paper No. 53075. in: The 2005 Annual meeting of ASAE, Tampa Florida, USA, July 17–20, 2005.

Lu, R., Ariana, D., 2002. near-infrared sensing technique for measuring internal quality of apple fruit. Applied Engineering in Agriculture 18 (5), 585–590.

Lu, R., & Chen, Y.R., 1998. Hyperspectral imaging for safety inspection of foods and agricultural products. In: Pathogen Detection and Remediation for safe eating – Proceedings in: The International Society for Optical Engineering, 3544, 121–133.

Lu, R., Peng, Y., 2006. Hyperspectral Imaging for assessing peach fruit firmness. Biosystems Engineering 93 (2), 161–171.

Kim, M.S., Lefcourt, A.M., Chao, K., Chen, Y.R., Kim, I., Chan, D.E., 2002a. Multispectral detection of fecal contamination on apples based on hyperspectral imagery: part I Application of visible and near-infrared reflectance imaging. Transactions of the ASAE 45 (6), 2027–2037.

Kim, M.S., Lefcourt, A.M., Chen, Y.R., Kim, I., Chan, D.E., Chao, K., 2002b. Multispectral detection of fecal contamination on apples based on hyperspectral imagery: Part II Application of hyperspectral fluorescence imaging. Transactions of the ASAE 45 (6), 2039–2047.

Martinsen, P., Schaare, P., 1998. Measuring soluble solids distribution in kiwi fruit using near infrared imaging spectroscopy. Post Harvest Biology and Technology 14 (3), 271–281.

Mehl, P.M., Chao, K., Kim, M., Chen, Y.R., 2002. Detection of defects on selected apple cultivars using hyperspectral and multispectral image analysis. Applied Engineering in Agriculture 18 (2), 219–226.

Mehl, P.M., Chen, Y.R., Kim, M.S., Chan, D.E., 2004. Development of hyperspectral imaging technique for the detection of apple surface defects and contaminations. Journal of Food Engineering 61 (1), 67–81.

Park, B., Abbott, J.A., Lee, K.J., Choi, C.H., Choi, K.H., 2003. Near-infrared diffuse reflectance for quantitative and qualitative measurement of soluble solids and firmness of Delicious and Gala apples. Transactions of the ASAE 46 (6), 1721–1731.

Ramma, I., Beni Madhu, S.P., Peerthum, S., 1999. Post harvest quality improvement of Banana, Food and Agricultural Research Council, Reduit. Mauritius.

Shmulevich, I., Galili, N., Howarth, M.S., 2003. Nondestructive dynamic testing of apples for firmness evaluation. Postharvest Biology and Technology 29 (3), 287–299.

Williams,P., Norris, K., 1987. Near Infrared Technology in the Agricultural and Food Industries. American Association of Cereal Chemists, Inc, St. Paul, MN.